Estimation of interplanetary plasma turbulence parameters from scintillations observations of quasars 3C 48 and 3C 298 near the minimum of solar activity

S.K. Glubokova, *S. A. Tyul'bashev,*
I. V. Chashei, V. I. Shishov

Pushchino Radio Astronomy Observatory,
Lebedev Physical Institute, Russian Academy of Science

The Solar Wind

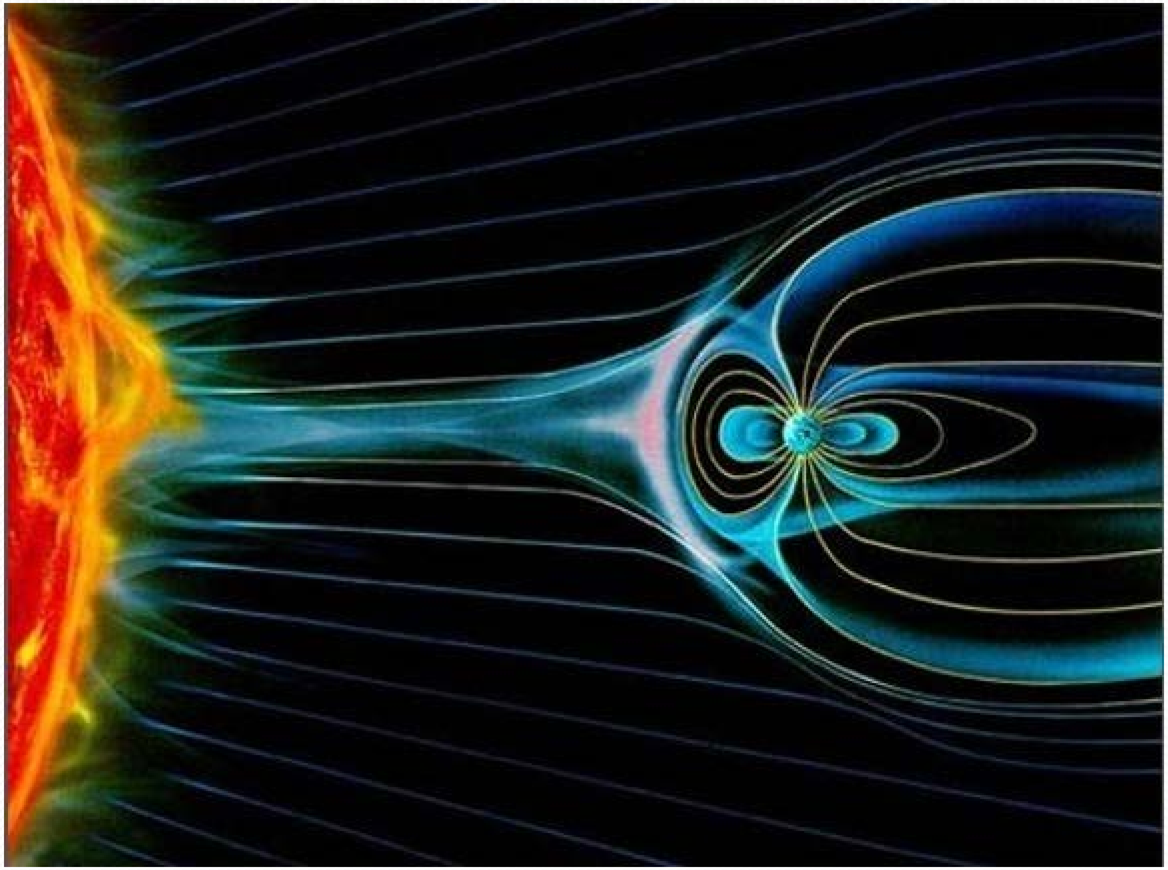

The extremely hot outer atmosphere of the Sun does not remain still. The Sun is continually emitting charged particles out into its surroundings that is collectively known as the solar wind. The realisation that something is always being expelled from the Sun came from observations of comets, auroras and geomagnetic storms.

The interplanetary scintillation (IPS)

Radio waves from space radio sources propagate through interplanetary plasma. The interplanetary scintillation (IPS) is fluctuation of space radio sources flux density, caused by fluctuation of interplanetary plasma density. Scintillation observations allow to derive information on solar wind spatial structure and large scale disturbances.

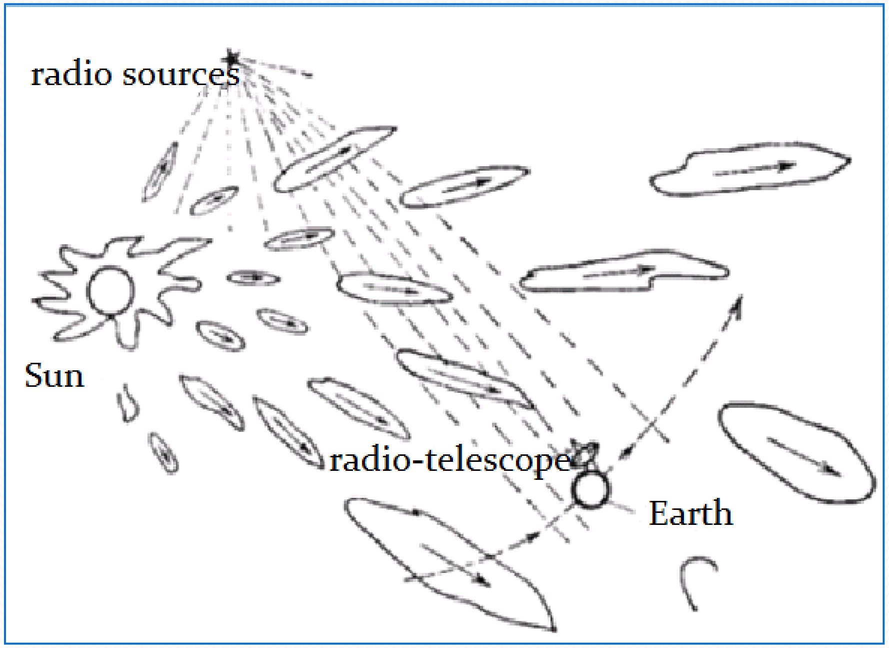

Compact ($<1''$) radio sources, such as active galactic nuclei (AGN) are used in IPS observations. The IPS characteristics are dependent only on source/observer geometry relative to the solar wind, and on the level of small scale density turbulence as well as on solar wind speed in the case of the point radio source. Sources angular sizes influence the IPS level and power spectra if sources have finite angular sizes. We presents the method and first results of turbulence spectral index, sources angular sizes and solar wind speed estimations. We shall concentrate below mainly on results concerning spectral index of turbulence spatial spectrum.

BSA FIAN

The scintillation observations are carrying out in monitoring regime by the radio telescope BSA (Big Scanning Array) of Lebedev Physical Institute from 2006 to present time.

Strong scintillating radio sources

Present work contains IPS data strong scintillating radio sources 3C048 and 3C298 near the minimum of solar activity cycle 23 (April-May 2007-2009 and November 2007-2009, respectively). These sources are strongest in our observations.

During the observation series the angular distance between the line of sight and the direction to the Sun (elongation) was in the limits 20^0-40^0.

Temporal IPS power spectra were calculated using initial records and then analyzed.

3C 048

Type QSO
Z =0.367000
B1950 01h34m49.8287s +32d54m20.161s
J2000 01h37m41.2994s +33d09m35.134s

3C 298

Type QSO
Z =1.437320
B1950 14h16m38.7809s +06d42m21.023s
J2000 14h19m08.1804s +06d28m34.805s

IPS temporal power spectra

IPS temporal power spectrum $P(f)$ is the Fourier transform of the correlation function $B_I(\tau)$:

$$P(f) = \int B_I(\tau) \exp(2\pi i f \tau)\, d\tau,$$

$$B_I(\tau) = \langle \delta I(t) \delta I(t+\tau) \rangle,$$

where $I(t)$ is the measured flux density and $\delta I(t) = I(t) - \langle I \rangle$ is it's temporal fluctuation.

IPS temporal power spectrum in the weak scintillation regime is defined by the following equation

$$P(f) = 4\lambda^2 \int \frac{A(z)}{v_{\perp(z)}} dz \int dq_{\perp} \Phi_e(q) \sin^2\left(\frac{q^2 z}{2k}\right) F^2(qz)\bigg|_{q_{\parallel}=\frac{2\pi f}{v_{\perp}(z)}}$$

where f- the temporal frequency, axis OZ is directed along the line of sight with $z = 0$ at the observation point, $A(z) = \frac{A_0}{(z^2+r_0^2)^2} \sim \frac{1}{r_0^4}$, $A_0 = 5 \cdot 10^{-25} cm^2$, $r_0 = \sin\varepsilon \cdot 1AU$, $v_{\perp}(z) = v\cos\varphi = v\frac{r_0}{\sqrt{r_0^2+z^2}}$ is the projection of the solar wind speed on the pattern plane at the point z, v is the solar wind speed, q - the spatial frequency, $q_{\parallel}$ - component of the spatial frequency along the projection of the solar wind velocity on the plane, $q_{\perp}$ - spatial frequency component of the perpendicular projection of the solar wind velocity on the plane, $q = \sqrt{q_{\perp}^2 + q_{\parallel}^2}$, $\Phi_e(q) = Cq^{-n}$ - spatial spectrum of electron density fluctuations in the interplanetary plasma, n is power exponent of $3D$ turbulence power spectrum, $k = \frac{2\pi}{\lambda}$ -is radio wavenumber, $F(q) = \left(\frac{1}{2\pi}\right)^2 \iint d^2\theta exp[-ikq\theta] I(\theta)$ is spatial spectrum of the radio source and $I(\theta)$ is brightness distribution of the source.

Numerical simulation of the temporal IPS spectra is performed in the following assumptions:

1) $3D$ spatial turbulence spectrum is isotropic power-low, $\Phi_e(q, q_z = 0) = Cq^{-n}$ with structure constant C;

2) the density turbulence level depends on heliocentric distance r as $C \sim r^{-4}$, $C = C_0\left(\frac{1AU}{r}\right)^4$;

3) the solar wind speed v is constant, radial and uniform;

4) the source brightness distribution over the source is a symmetric Gaussian $I(\theta) = exp\left(-\frac{\theta^2}{2\theta_0^2}\right)$ with angular radius θ_0 at the $\frac{1}{e}$ level.

The model used in simulations has four free parameters: absolute turbulence level Co , solar wind speed v, turbulence spectral index n and radio source size θo. First three of them can change from day to day, and last one is assumed to be constant. We define free parameters from the best fitting of calculated spectrum P(f) into spectrum obtained from IPS measurements.

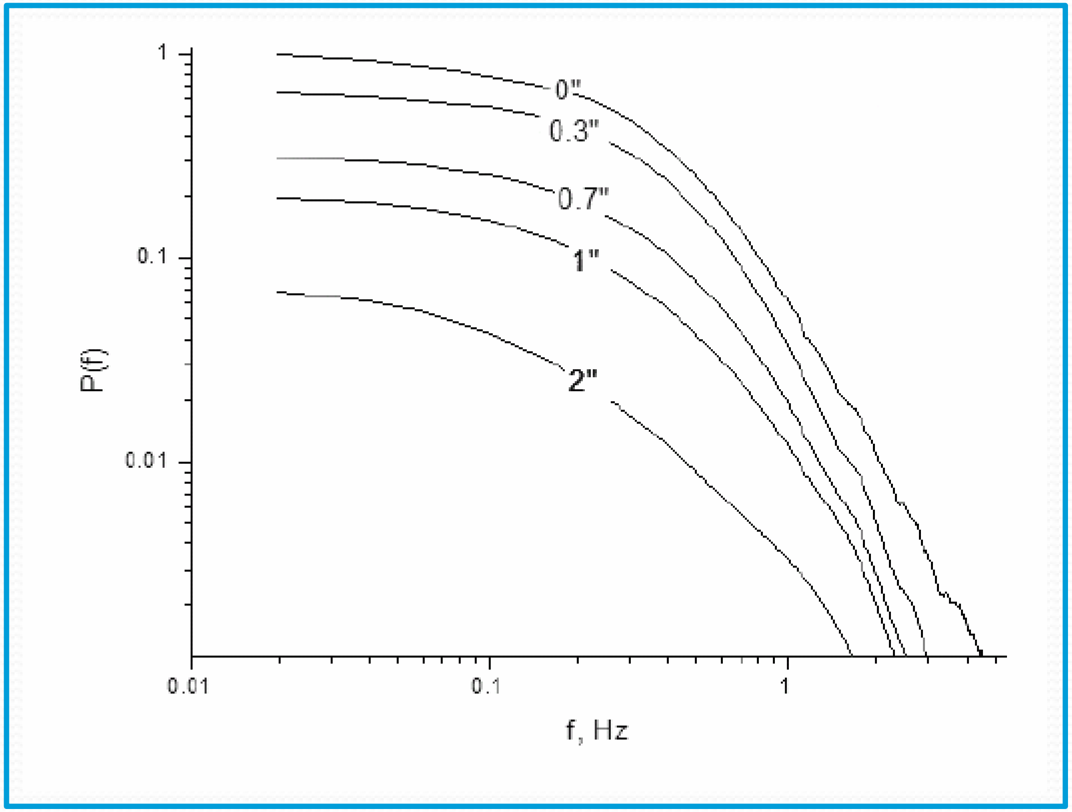

The theoretical spectra of the scintillation for different angular sizes of sources (n=3.6, v=400 km/s)

Figure presents results from these numerical computations. The angular size of the source exerts an appreciable influence at high frequencies. Therefore, the larger the range of observed wavelengths available for analysis, the more confidently a source angular size can be measured.

The examples of IPS records for the sources 3C 048 and 3C 298

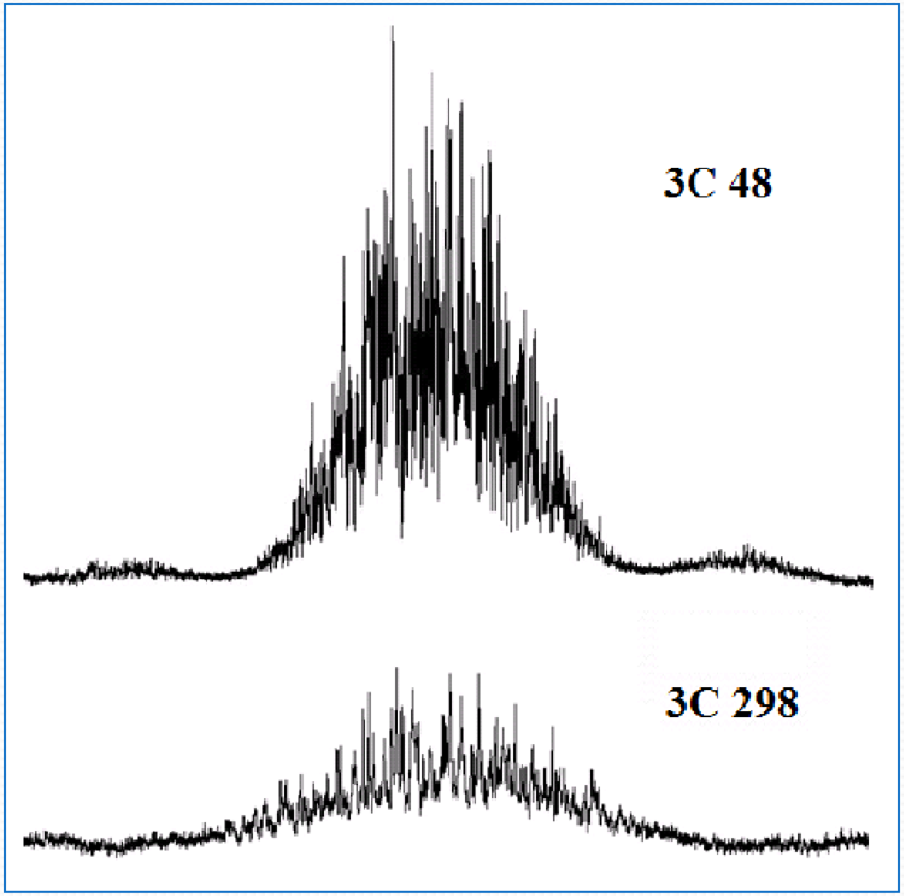

Signal-to-noise ratio for the source 3C 48 is significantly higher than for 3C 298. Good records for 3C 48 is much larger, so all dependencies we show primarily for 3C 48.

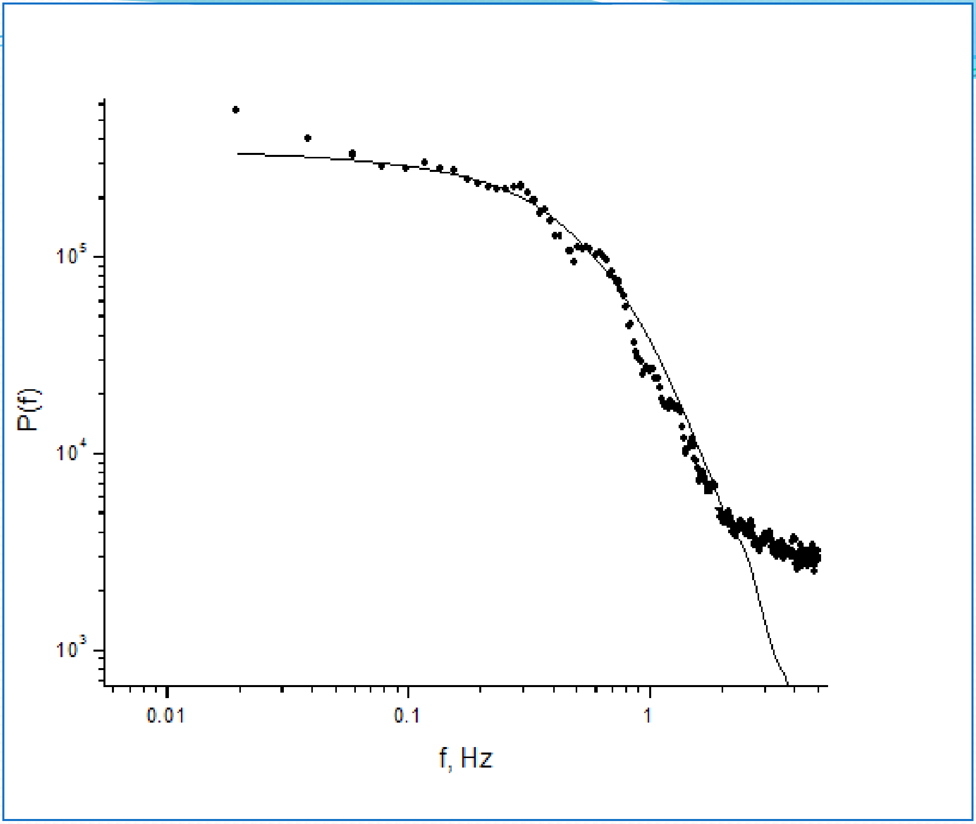

A sample of the power spectrum of the source 3C 48(dots) and inscribed the theoretical power spectrum (full line) n=3.74, v=520 km/s.

Fitting procedure is illustrated by figure. The measured IPS temporal power spectrum shown in figure has typical shape with approximately constant level at low frequency and roll off approximately exponentially at high frequencies. Constant level at highest frequencies corresponds to the noise.

Simulation results

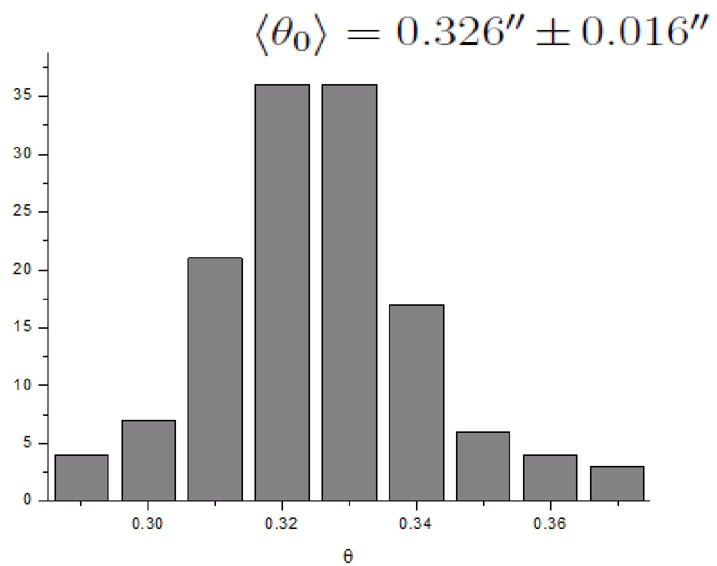

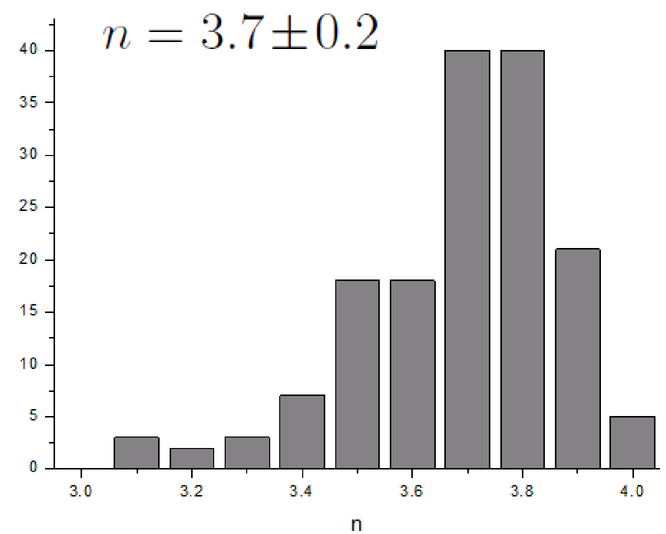

The histogram for distribution of angular sizes of 3C 48.	The histogram for distribution of values of index of turbulent plasma.

- The distribution of the source angular sizes for 3C 48 is shown in left figure. Using this distribution one can find the mean value. This result agrees well with the results of other authors.
  Further the source size is assumed to be constant and equal to θ0 = 0.326″ and other free parameters are defined for each IPS record. The distribution of the turbulence spectral index n is presented in right figure. From this distribution we find mean value n = 3.7 ± 0.2, the observed values of n are in the limits 3.1 − 4.0.
  The records of the source 3C 298 have not satisfactory quality signal-to-noise ratio, so the value of the angular size is taken from the literature (θ0 = 0.25”). The value of the turbulence spectral index n will be driven for the same reason. Therefore, for source 3C 298 we obtain only qualitative relations.

Analyze the results of the spectral index of turbulence n, in order to try to select the model which describes the IPS.

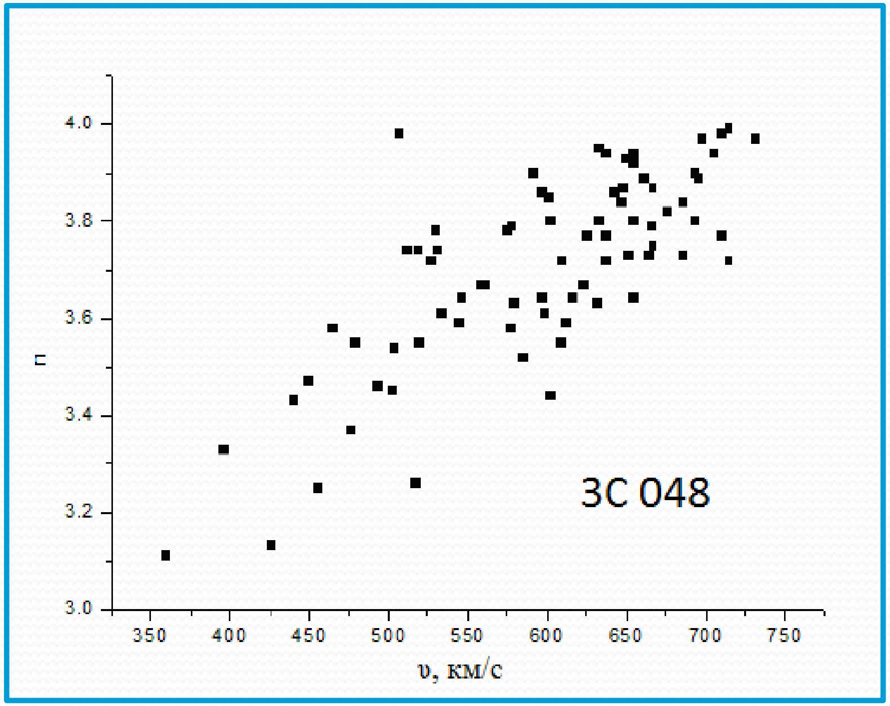

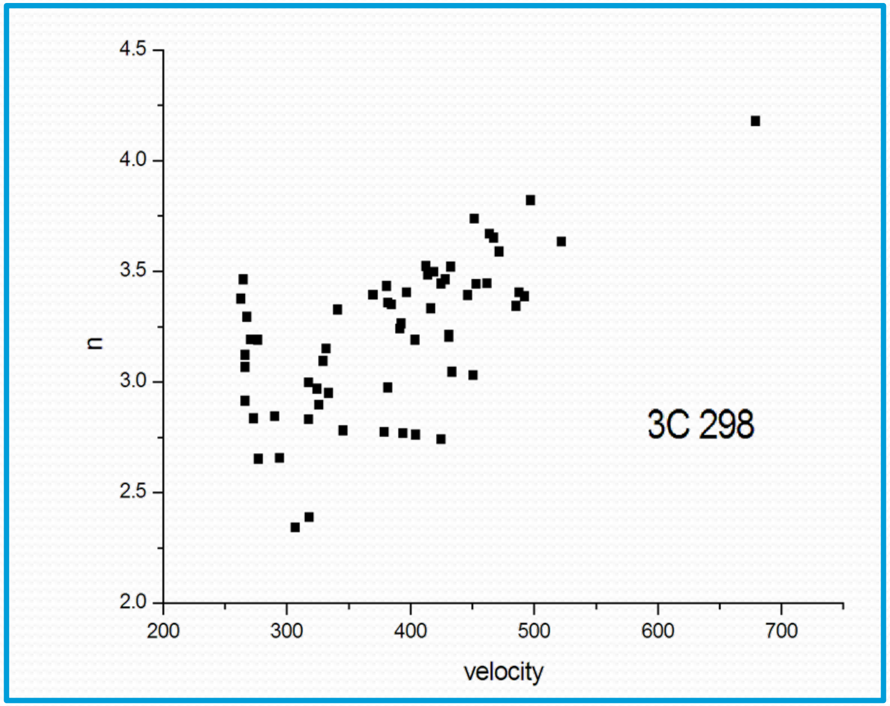

Dependence of the index of plasma turbulence on the solar wind velocity.

The slow solar wind plasma corresponds to lower spectral values index of turbulence and rapid - to large values of the index.

This physical dependence is observed the first time. It is the same for 3C 48 and 3C 298. Next, we check how to explain this relationship.

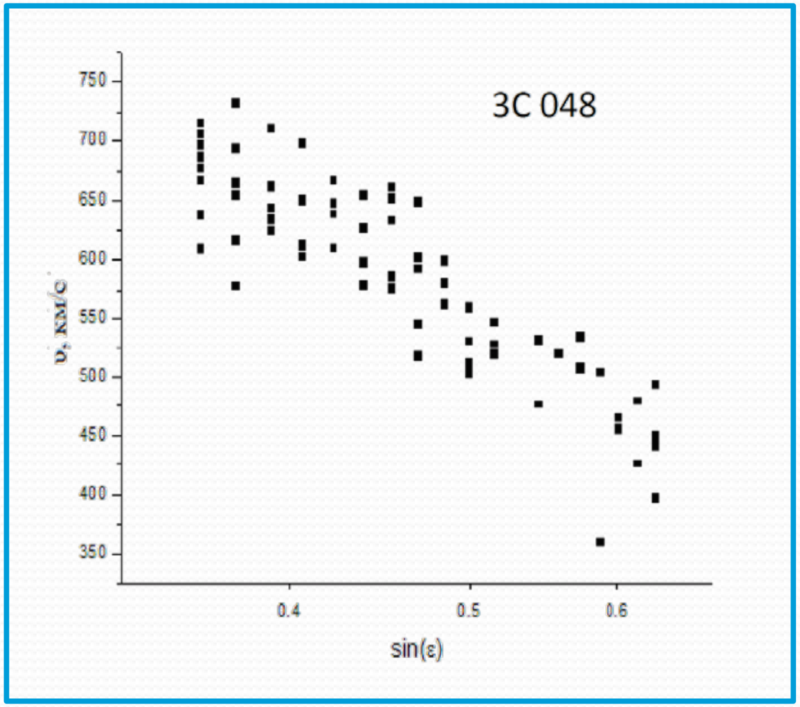

Dependence of the solar wind velocity on elongation. On the x-axis is logarithmic scale.

This result can be explained by a typical for period of minimum solar activity stable bimodal structure of solar wind. At low heliolatitude wind is slow and fast, less dense wind is at middle and high heliolatitude.

We now know that the number of sunspots on the Sun varies during a cycle lasting about 11 years. A time of many sunspots is called a sunspot maximum. During a sunspot minimum, the Sun is almost devoid of sunspots. This regular variation is known as the 11-year sunspot cycle.

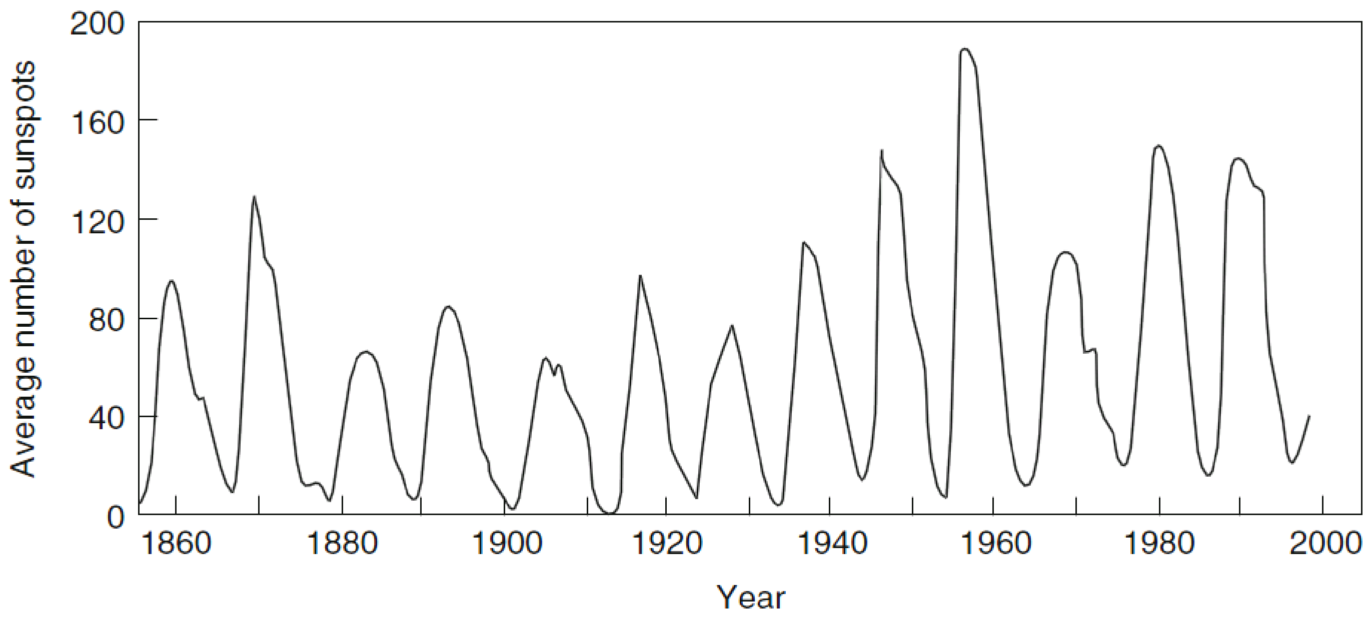

Graph showing how the average number of sunspots for each year has varied since 1850. The cycle of maximum and minimums has an 11-year period.

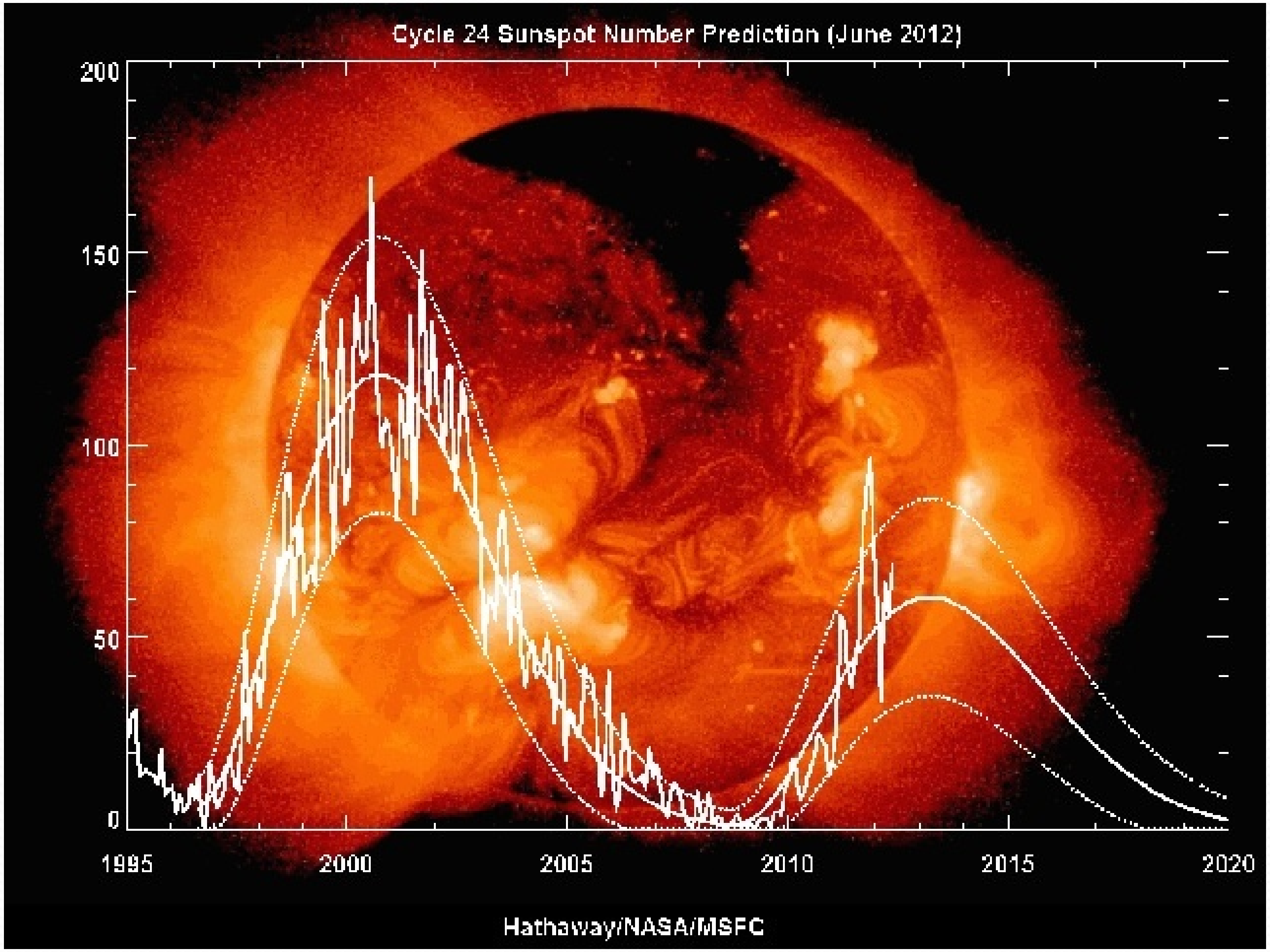

Cycle 24 Sunspot Number Prediction (June 2012)
200
150
100
50
0
1995
2000
2005
2010
2015
2020
Hathaway/NASA/MSFC

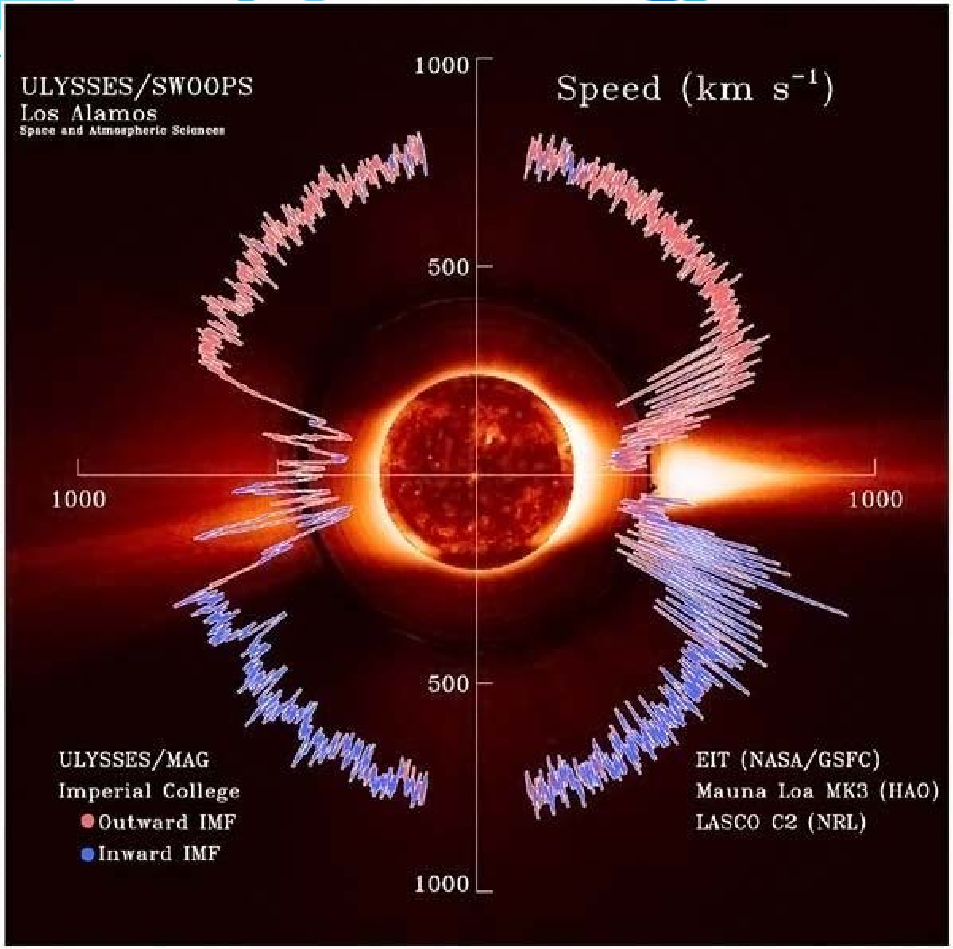

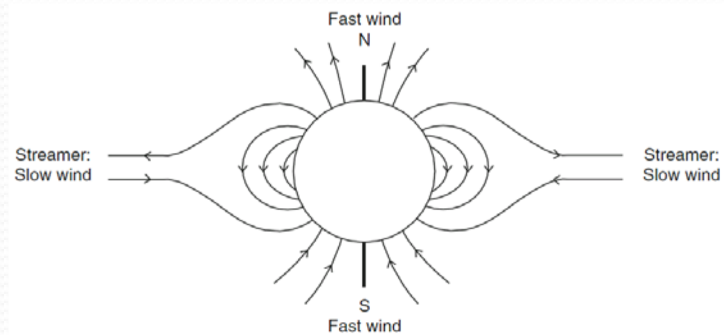

Magnetic field lines around the Sun at a time of solar minimum.

At solar minimum the fast wind escapes from the Sun along the open magnetic field lines of polar coronal holes. The slow wind originates from the equatorial region in coronal streamers, where the magnetic field lines are closed close to the Sun and oppositely directed and parallel further from the Sun.

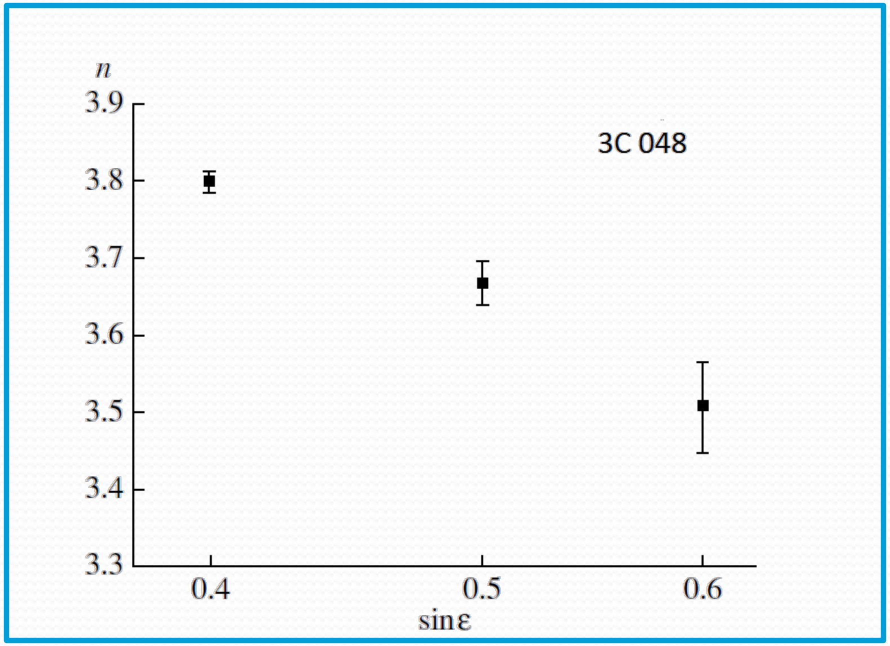

Dependence of the values of the spectral index of plasma turbulence on elongation. On the x-axis is logarithmic scale.

There is a clear downward trend in the spectral index of the turbulence on elongation.

Bimodal structure of the solar wind

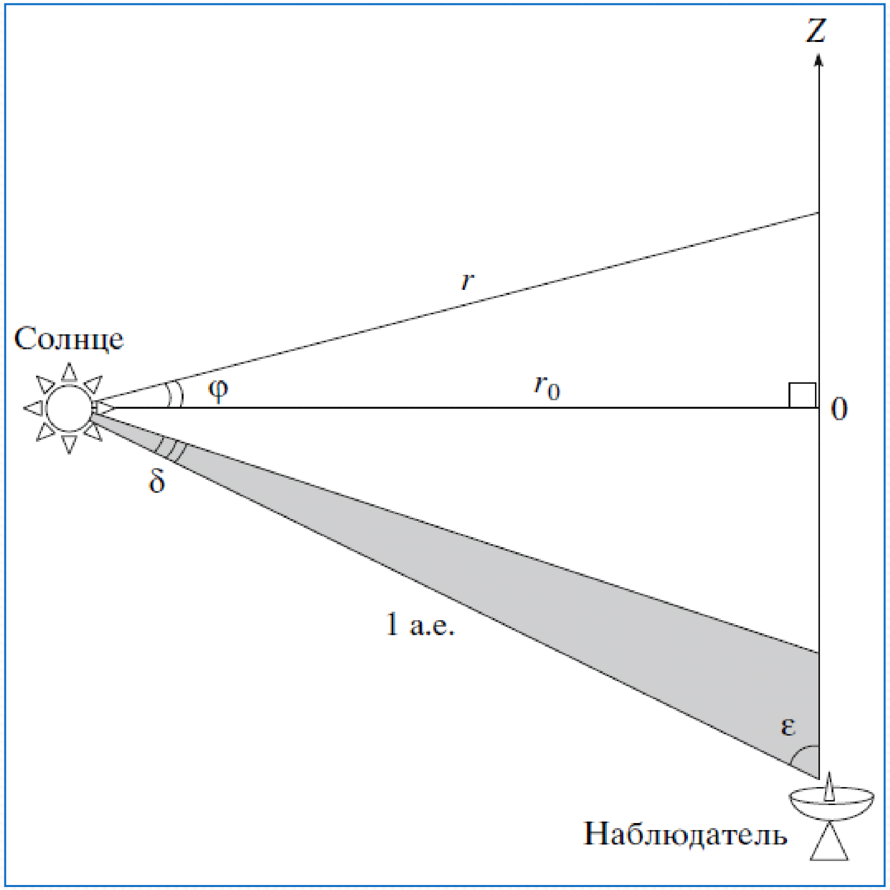

As can be seen from the numerous data this latitudinal structure occurred during the observations 2007-2009 near a minimum 23/24 cycle of solar activity.

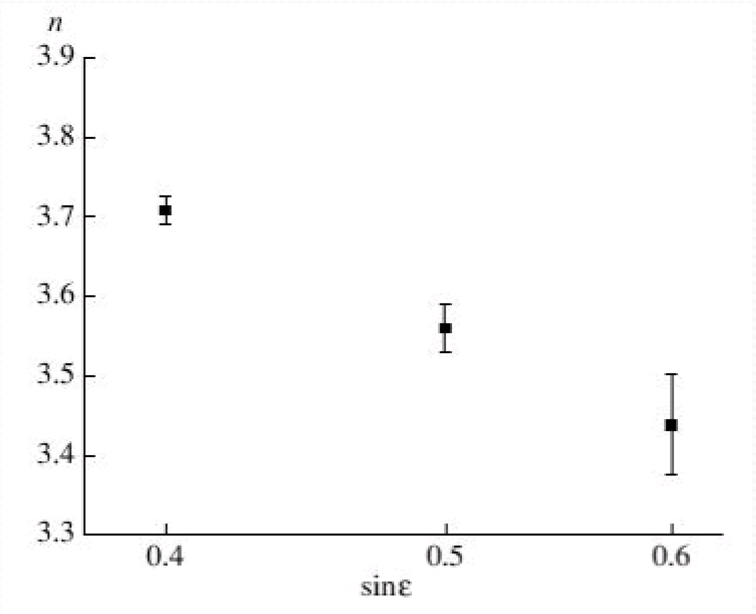

Dependence of the values of the spectral index of plasma turbulence on elongation with the bimodal structure of the solar wind. On the x-axis is logarithmic scale.

- There is no significant differences in the dependence of the index of plasma turbulence on elongation of the experimental points and the theoretical curve. So the bimodal structure of the solar wind on the elongations (elongations are 20-40), isn't significantly affect the resulting dependence of the spectral index for the turbulence.
- Thus, the dependence of the index of turbulence on the solar wind velocity is, apparently, a real effect.

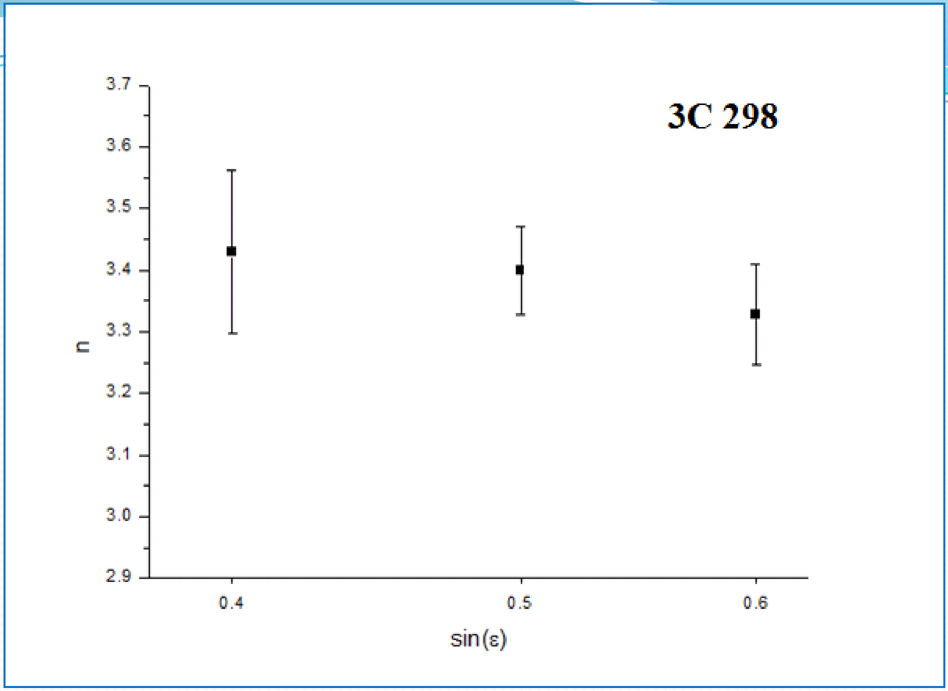

Dependence of the values of the spectral index of plasma turbulence on elongation. On the x-axis is logarithmic scale.

The source 3C 298 is multi-components, the components are aligned and the distance between the components is such that it is difficult to describe the source by a simple model. We can put additional parameters in the model which we used: the elongation of the details, the distance between the components, the angular size of each component, taking into account the relative details position of the source relative to the direction of the solar wind. However, with such a model cannot be obtain a unique solution. We suppose that the obtained values of the turbulence spectral index which are lower than for the source 3C 48 are connected with a complex angular structure of the source 3C 298.

The problem of physical processes responsible for formation of wide power-law spectrum in inertial spectral range and energy cascading from turbulence outer scale to dissipation spectral range is still unsolved. Our data do not allow distinguishing between Kolmogorov (**n = 11/3**) and Iroshnikov/Kraichnan (**n = 7/2**)spectra because both models are in agreement with measurements within the error limits. The above preliminary results show that the spectrum of turbulence can be different for different types of flows. In the fast solar wind spectrum of small-scale turbulence near the Kolmogorov, and in the slow - to the spectrum Iroshnikov/Kraichnan.

Future studies based on more rich statistics with large scale and small scale data comprehensive comparison are needed for convincing conclusions.

Conclusions

- These results indicate that the density turbulence spectral index n found from IPS data decreases in the transition from high-latitude solar wind speed in the slow low-latitude. The dependence of the spectral index of the turbulence on the speed of the solar wind is a real effect, and not due to the influence of the bimodal structure in the period of minimum solar activity.

- This conclusion can be useful for developing of new models of the solar wind turbulence.

Thank you!